



Published in final edited form as:

Nature. 2014 February 20; 506(7488): 387–390. doi:10.1038/nature12891.

Convergent Evolution of a Fused Sexual Cycle Promotes the Haploid Lifestyle

Racquel Kim Sherwood^{#1,2}, Christine M. Scaduto^{#1}, Sandra E. Torres^{1,3}, and Richard J. Bennett^{1,#}

¹Department of Microbiology and Immunology, Brown University, 171 Meeting St, Providence, RI, 02912.

These authors contributed equally to this work.

Sexual reproduction is the prerogative of eukaryotic species and involves the fusion of haploid gametes to form a diploid cell that subsequently undergoes meiosis to generate recombinant haploid forms. This process has been extensively studied in the unicellular yeast *Saccharomyces cerevisiae*, which exhibits separate regulatory control over mating and meiosis. Here we address the mechanism of sexual reproduction in the related hemiascomycete species *Candida lusitaniae*. We demonstrate that in contrast to *S. cerevisiae*, *C. lusitaniae* exhibits a highly integrated sexual program in which the programs regulating mating and meiosis have fused. Profiling of the *C. lusitaniae* sexual cycle revealed that gene expression patterns during mating and meiosis were overlapping, suggestive of co-regulation. This was particularly evident for genes involved in pheromone MAPK signaling, which were highly induced throughout the sexual cycle of *C. lusitaniae*. Furthermore, genetic analysis showed that the ortholog of *IME2*, a ‘diploid-specific’ factor in *S. cerevisiae*^{3,4}, and *STE12*, the master regulator of *S. cerevisiae* mating^{5,6}, were each required for progression through both mating and meiosis in *C. lusitaniae*. Together, our results establish that sexual reproduction has undergone significant rewiring between *S. cerevisiae* and *C. lusitaniae*, and that a concerted sexual cycle operates in *C. lusitaniae* that is more reminiscent of the distantly related ascomycete, *Schizosaccharomyces pombe*. We discuss these results in light of the evolution of sexual reproduction in yeast, and propose that regulatory coupling of mating and meiosis has evolved multiple times as an adaptation to promote the haploid lifestyle.

Sexual reproduction is divided into two programs: gamete fusion, in which haploid cells merge to form a diploid cell, and gametogenesis, in which a specialized cell division, meiosis, generates recombinant haploid gametes. Sexual reproduction in *S. cerevisiae* involves mating between cells of opposite mating type, generating diploid products⁷ that

Users may view, print, copy, download and text and data- mine the content in such documents, for the purposes of academic research, subject always to the full Conditions of use: http://www.nature.com/authors/editorial_policies/license.html#terms

Correspondence: Richard_Bennett@brown.edu.

²Current Address: Department of Microbial Pathogenesis, Yale University, 295 Congress Avenue, New Haven, CT, 06536-0812.

³Current Address: University of California San Francisco, 1700 4th St, San Francisco, CA 94158-2330.

Author Contributions

R.K.S. and C.S. constructed strains, analyzed phenotypes, and performed transcriptional profiling experiments. S.T. and R.J.B. constructed strains and analyzed phenotypes. R.K.S., C.S., and R.J.B. were involved in study design and writing of the manuscript.

subsequently undergo meiosis upon nutritional limitation^{1,8}. It is unclear, however, how representative this sexual cycle is of that in other yeast species. Here, we examine regulation of sexual reproduction in the related hemiascomycete *Candida lusitanae*, a member of the *Candida* clade of human pathogens⁹. *C. lusitanae* was recently shown to have a complete sexual cycle despite lacking orthologs of key meiosis genes such as *IME1*, encoding the master transcriptional regulator of meiosis in *S. cerevisiae*⁹⁻¹¹. In addition, whereas *S. cerevisiae* is predominantly diploid, *C. lusitanae* cells preferentially exist in the haploid form and therefore exhibit a transient diploid state^{9,10}.

Transcriptional profiling of *C. lusitanae* cells progressing through mating and meiotic programs was performed and compared to those of *S. cerevisiae*. In total, 406 genes were induced >4-fold during *C. lusitanae* mating, including highly conserved MAPK genes that regulate pheromone signaling in diverse fungal species^{2,12,13} (Fig. 1a and Extended Data Fig. 1). Interestingly, we also observed elevated expression of several genes that are orthologs of ‘meiosis-specific’ genes in *S. cerevisiae*, including *SPO11*, *REC8*, and *IME2*^{3,14,15,16} (Fig. 1a). We similarly performed expression profiling on *C. lusitanae* diploid a/a cells induced to enter meiosis. Cells became enlarged by 8 h, exhibited a morphological change by 12 h, and by 18-36 h dyad (2-cell) spores were formed, as is typical of this species¹⁰ (Extended Data Fig. 2a-c). Profiling revealed that a total of 618 genes were induced during *C. lusitanae* meiosis, compared to 480 genes during *S. cerevisiae* meiosis¹⁷. In *S. cerevisiae*, meiotic gene expression includes early, middle, and late stages of expression¹⁷. We were similarly able to distinguish three temporal classes of meiotic gene expression in *C. lusitanae* (Fig. 1b and d, and Extended Data Fig. 2d). In total, we observed increased expression (>3-fold) of 255 early genes, 307 middle genes, and 56 late genes during *C. lusitanae* meiosis (Fig. 1e). Thus, despite lacking an ortholog of *IME1*, many downstream components of meiosis are regulated in a similar stage-specific manner in *C. lusitanae* as in *S. cerevisiae*.

The most striking aspect of *C. lusitanae* meiosis was the expression of many genes whose orthologs are expressed specifically during mating in *S. cerevisiae*. In particular, multiple components of the pheromone MAPK signaling cascade were highly induced, including the terminal transcription factor *STE12* (Fig. 1c and f). In addition to MAPK genes, pheromone, pheromone receptor, and pheromone processing genes were also induced in *C. lusitanae* meiosis (Extended Data Fig. 1). We therefore surmised that MAPK signaling might play a role in regulating *C. lusitanae* meiosis, in addition to its conserved function in directing cell-cell communication and conjugation.

Given that program-specific expression of many *S. cerevisiae* mating and meiosis genes does not occur in *C. lusitanae* orthologs, genetic experiments were performed to determine whether this transcriptional rewiring has functional consequences for the sexual cycle. First, the role of *C. lusitanae* *Ime2* in mating and meiosis was analyzed. *S. cerevisiae* *Ime2* (Inducer of meiosis 2) is a conserved serine/threonine kinase that acts in tandem with the cyclin-dependent kinase Cdk1 to promote meiosis^{3,4,18,19}. As predicted based on *IME2* function in *S. cerevisiae*, loss of *IME2* (CLUG_00015) in *C. lusitanae* blocked meiosis; wildtype diploid cells formed haploid progeny with ~40% efficiency after 3 days, whereas <1% of haploids were formed by *ime2 /ime2* cells (Fig. 2a). In addition, whereas wildtype

diploids generated dyad spores, *ime2 /ime2* mutants failed to sporulate (Fig. 2b). These results establish a conserved role for *IME2* in regulating meiosis in hemiascomycete yeast, even in species for which *IME1* is absent. Profiling of *C. lusitaniae ime2 /ime2* mutants revealed that most early meiosis genes were still induced in this background, while induction of many middle and late meiosis genes was lost (Extended Data Fig. 3). We also note that induction of *NDT80* (*CLUG_05634*) and genes encoding cell cycle regulators was compromised in the *ime2 /ime2* mutant (Extended Data Fig. 3b). *NDT80* is responsible for the induction of middle meiosis genes in *S. cerevisiae*, where its expression is dependent on *Ime2*²⁰. The diminished expression of *NDT80*, together with the loss of expression of cell cycle genes, is likely responsible for the inability of *C. lusitaniae ime2 /ime2* cells to proceed through meiosis.

We next addressed the role of *IME2* in *C. lusitaniae* mating. In contrast to *S. cerevisiae* where *IME2* has no role in mating, *C. lusitaniae IME2* was induced during mating (Fig. 2c) and was required for the efficient formation of mating products. Thus, co-incubation of *C. lusitaniae a* and α cells resulted in approximately 0.5% of cells forming *a*/ α diploids, while bilateral crosses between *ime2 a* and *ime2* α cells resulted in a mating frequency of less than 0.03% (a 16-fold decrease, Fig. 2d). Unilateral crosses between wildtype and *ime2* mutants showed mating frequencies similar to those between wildtype partners (Fig. 2d). Complementation by reintegration of the *IME2* gene into the mutant background restored mating competency in the bilateral cross (Extended Data Fig. 4). These results establish a novel role for *IME2* in *C. lusitaniae* mating, and indicate that the *ime2* defect is limited to bilateral crosses. The latter observation is consistent with a late role for *Ime2* during mating following the fusion of *a* and α partner cells. Microscopic analysis of *ime2* crosses showed the formation of zygote structures further supporting a late role for *Ime2* during mating (Fig. 2e), and additional studies will be required address the precise role of *Ime2* in this process.

Next, we investigated the role of pheromone MAPK signaling and the transcription factor *Ste12* in the *C. lusitaniae* sexual cycle. First, we tested whether *C. lusitaniae* cells undergoing meiosis actively secrete pheromone. A pheromone reporter assay was developed in which the *C. lusitaniae* α pheromone receptor was heterologously expressed in the related species *Candida albicans* (Fig. 3a). Such heterologous expression of receptors has been shown to result in successful signaling in response to species-specific pheromones²¹. Co-incubation of the GFP-labeled reporter strain with *C. lusitaniae* cells undergoing meiosis showed induction of a morphological response in the reporter cells (Fig. 3b), demonstrating that *C. lusitaniae* cells are actively secreting α pheromone during meiosis.

STE12 is the master regulator of mating and pheromone signaling in *S. cerevisiae* and many other hemiascomycetes, including *Candida* species^{2,12}. To test the role of *STE12* in the sexual cycle of *C. lusitaniae* we constructed haploid and diploid *ste12* mutants. Loss of *STE12* (*CLUG_02576*) in haploid cells led to a complete block in zygote formation and mating between *a* and α cells (Fig. 3c, 3d), as expected based on previous studies²². Surprisingly, however, loss of *STE12* in *C. lusitaniae a*/ α diploids also led to a block lock in meiosis and sporulation. Thus, formation of meiotic progeny was reduced ~100-fold in *ste12 /ste12* mutants (Fig. 3e) and spore formation was abolished (Fig. 3f and Extended Data Fig. 2c). Reintegration of the *STE12* gene into the *ste12 /ste12* background restored

the ability to undergo meiosis (Extended Data Fig. 5). Expression profiling revealed that the meiotic transcriptional profile was essentially absent from *ste12* /*ste12* mutants (Fig. 3g). Our results therefore establish that *STE12* plays a critical role in regulating *both* mating and meiosis in *C. lusitaniae*, in contrast to *S. cerevisiae* where *STE12* specifically regulates mating only.

Taken together, our studies demonstrate that a fundamental rewiring of the sexual cycle has occurred between the two hemiascomycetes, *S. cerevisiae* and *C. lusitaniae*. Mating and meiosis are distinct programs in *S. cerevisiae*, yet these programs are integrated in *C. lusitaniae* (Fig. 4a and Extended Data Fig. 7). This is evident both from transcriptional profiles that reveal overlap of gene expression patterns in mating and meiosis, as well as genetic analysis of key regulators of the sexual cycle. In particular, whereas *STE12* and *IME2* are necessary for *S. cerevisiae* mating and meiosis, respectively, the *C. lusitaniae* orthologs are required for efficient progress through both stages of the sexual cycle.

The regulation of sexual reproduction in *C. lusitaniae* exhibits striking parallels to that in the distantly related ascomycete *S. pombe*, even though these lineages diverged from one another more than 330 million years ago²³. In *S. pombe*, mating and meiosis are also tightly coupled and both are dependent on pheromone MAPK signaling and the downstream transcriptional regulator, Ste11^{24,25}. In *C. lusitaniae*, we show that the pheromone MAPK-associated transcription factor *STE12* is similarly essential for both mating and meiosis. Thus, in both *S. pombe* and *C. lusitaniae* the programs regulating mating and meiosis are fused (Fig. 4a).

To address if Ste12 also regulates meiosis in other hemiascomycete species, we deleted the *STE12* ortholog from related sexual species including *S. cerevisiae*, *Kluyveromyces lactis*, *Pichia pastoris*, and *Yarrowia lipolytica* (Extended Data Fig. 6). In each species loss of *STE12* failed to block meiosis, suggesting that the meiotic function of *STE12* evolved relatively recently in the *C. lusitaniae* lineage (Fig. 4b). In support of this hypothesis we note that *C. lusitaniae*, but not the other hemiascomycete species, lost the transcriptional regulator $\alpha 2$ during evolution^{9,10}. The $\alpha 2$ gene acts to prevent expression of haploid-specific genes (including MAPK genes) in diploid **a/a** cells in diverse yeast species^{26,27}. Thus, as previously hypothesized^{9,10}, the loss of $\alpha 2$ could have preceded the rewiring of meiotic control in *C. lusitaniae*. In particular, we propose that it facilitated MAPK signaling and enabled Ste12 to assume control of meiosis in this species.

Why have such distinct modes of sexual regulation evolved in diverse unicellular yeast? The most parsimonious explanation is that these differences reflect a species' preference for one ploidy state over another. Both *C. lusitaniae* and *S. pombe*, despite being highly divergent, exhibit haploid lifestyles that contrast sharply with the predominantly diploid lifestyle of *S. cerevisiae*. Co-regulation of the transcriptional programs controlling mating and meiosis therefore ensures that cells, once mated, immediately enter meiosis and return to the haploid state. This could represent an adaptive advantage for haploid cells in both *C. lusitaniae* and *S. pombe*. Alternatively, the selective pressure to keep these two sexual programs separate may have been lost during evolution, leading to the amalgamation of these programs in the two species. While the relative advantages of haploidy and diploidy continue to be

debated^{28,29}, it is clear that distinct transcriptional circuits can evolve to promote either haploid or diploid lifestyles. That this mode of regulation evolved independently in *S. pombe* and *C. lusitaniae* further suggests that examples of fused sexual cycles will be found throughout the fungal tree of life.

Methods

Media and Reagents

Standard laboratory media were prepared as previously described³¹. Potato dextrose agar (PDA) was prepared as a 10% dilution of standard PDA medium (Becton Dickinson) that was solidified using 1.45% Bacto Agar (Becton Dickinson)³². Nourseothricin-resistant transformants were selected on YPD (yeast peptone dextrose) medium containing 200 µg/ml nourseothricin, as previously described³³. Kanamycin-resistant transformants were selected on YPD medium supplemented with 50 µg/ml kanamycin. Liquid yeast peptone sorbitol (YPS) was prepared similar to YPD, however 2% sorbitol was used in the place of dextrose. Haploid progeny from sporulation assays were selected on YPD medium supplemented with 10 µg/ml cycloheximide¹⁰. SC-Maltose consisted of synthetic complete medium supplemented with 2% maltose. Malt medium (2% malt extract, 3% agar) was used to induce mating and meiosis in *K. lactis*. *Pichia pastoris* mating/sporulation medium consisted of sodium acetate medium (0.5% sodium acetate, 1% KCl, 1% glucose, 2% agar³⁴). *Yarrowia lipolytica* sporulation was achieved using V8 sporulation medium (40% V8 juice, 0.8% yeast extract, 1.6% agar, pH 6.5).

C. lusitaniae transformations

For *C. lusitaniae* strains, three transformation protocols yielded mutant strains in this study. In the first protocol, cells from overnight cultures were diluted into 50-100 ml liquid YPD cultures. Cultures were grown overnight and harvested at a final OD₆₀₀ of 1.7-1.8. Cells were pelleted and resuspended in a transformation buffer composed of: 1 X Tris EDTA, 0.1 M lithium acetate, 0.01 mM dithiothreitol to a final volume of 20 ml. Cells were incubated in a roller for one hour at 24°C, washed twice with ice-cold water, once with ice-cold 1 M sorbitol and resuspended in 100 µl of 1 M sorbitol. 40 µl of cells and 5 µg of construct DNA were added to a 0.2 mm electroporation cuvette (BioRad). Cells were electroporated at 1.8 kv (BioRad MicroPulser) and immediately resuspended in 1 ml ice-cold sorbitol. Cells were pelleted and allowed to recover for 4 h in a 50/50 mix of YPD and YPS. Cells were plated onto YPD supplemented with nourseothricin for transformant selection^{10,22,35,36}.

In an alternate protocol, transformations were performed when target genes were highly expressed during sporulation or nutritional starvation. To accomplish this, 6×10^7 diploid *C. lusitaniae* cells were plated onto PDA and subsequently harvested when targeted genes were highly induced (after 10-14 h of sporulation). Cells were rinsed from PDA plates with water, pelleted, and incubated in transformation buffer. The remainder of the protocol was completed as described above. Finally, RSY575 and CAY4240 were generated using a previously described protocol³⁷.

Strain Construction

All strains constructed for this study are listed in Supplemental Table 1, and oligonucleotides used are listed in Supplemental Table 2. Strain RSY148 was genetically marked by deleting both *ARG4* and *ADE2* genes. To accomplish this, the 5' flank of *ARG4* was PCR amplified with oligonucleotides RS84/RS85. The 3' flank of *ARG4* was amplified with oligonucleotides RS86/RS87. The 5' flank was digested with *ApaI* and *XhoI* and ligated between *ApaI* and *XhoI* sites in pSFS2a³³. Next, the *ARG4* 3' flank was digested with *PstI* and *NotI* and ligated between the same sites within the plasmid containing the 5' flank of *ARG4*. This construct (pRB243) was linearized with *ApaI* and *NotI* and transformed into RSY148 to create RSY289. Integration was checked by PCR across the 5' and 3' gene boundaries using oligonucleotides RS90/BL70 and BL71/RS91, respectively. Loss of the *ARG4* open reading frame was confirmed by PCR using oligonucleotides RS88/RS89. RSY289 was cultured on SC-Maltose to induce expression of the *MAL2* promoter resulting in expression of *caFLP* and excision of the *SATI* cassette at the FRT sites³³ creating RSY297. Loss of the *SATI* marker from the deletion construct was confirmed by PCR analysis using RS90 and BL70.

ADE2 was deleted from RSY297 by PCR amplifying the 5' flank of *ADE2* using oligonucleotides RS230/RS231 and the product ligated between *ApaI* and *XhoI* sites in pSFS2a. The 3' flank of *ADE2* was PCR amplified using oligonucleotides RS228/RS229 and ligated into the plasmid using *NotI* and *SacII*, generating pRB243. The *ADE2* deletion cassette was generated with *ApaI* and *SacII* and transformed into RSY297 to create RSY379. Correct integration of the construct was verified by PCR analysis across the 5' and 3' junctions using oligonucleotides RS226/BL70 and BL71/RS227. Loss of the *ADE2* ORF was confirmed by PCR using oligonucleotides RS276/RS277. RSY379 was cultured on SC-Maltose to induce excision of the *SATI* cassette to generate RSY411.

IME2 deletions were constructed in **a** and **α** strains RSY411 and RSY284, respectively. The 5' flank of *IME2* was PCR amplified using oligonucleotides RS224/RS265 and cloned into pSFS2a with *KpnI* and *ApaI*. Next, the 3' flank of *IME2* was PCR amplified using oligonucleotides RS263/RS225. The pSFS2a plasmid containing the 5' flank of *IME2* and the 3' *IME2* PCR product were digested with *NotI* and *SacII* and ligated to generate pRB245. pRB245 was linearized with *KpnI* and *SacII* and transformed into RSY284 to generate *ime2* strain RSY410. The same construct was transformed into RSY411 creating *ime2* strains RSY406, RSY407, and RSY408. Accurate integration of the construct was confirmed by PCR across 5' and 3' junction boundaries using oligonucleotides RS167/BL70 and BL71/RS148. Loss of *IME2* was verified by PCR analysis using oligonucleotides RS165/RS166. RSY410 was cultured on SC-Maltose to induce excision of the *SATI* cassette creating RSY437. To reintegrate *IME2* at the endogenous locus the *IME2* ORF, together with ~ 1 kb of promoter, was PCR amplified using primers RS281 and RS282. The PCR product was digested with *KpnI* and *XhoI* and cloned into pSFS2a to generate plasmid pRB278. pRB278 was linearized using *PshAI* and transformed into RSY437. Integration at the endogenous *IME2* locus was checked by PCR using primers RS224/BL70. Diploid *ime2/ ime2* strains RSY427, RSY428 and RSY429 were generated by mating haploid

RSY406 and RSY410 strains. Strains were verified by flow cytometry, PCR verification of *MTL a/a* configuration, and prototrophy.

Diploid *STE12* mutant strains were constructed in RSY432. The 5' flank of *STE12* was PCR amplified using oligonucleotides RS323/RS324. The 5' flank and pSFS2a were digested with *KpnI/ApaI* and ligated. The 3' flank of *STE12* was PCR amplified using oligonucleotides RS325/RS326 and integrated into this vector using *NotI/SacII*. The *STE12* deletion construct was excised with *KpnI/SacII* and transformed into RSY432 to generate independent *STE12/ste12* heterozygous strains RSY541 and RSY575. RSY541 and RSY575 were incubated on SC-Maltose to induce excision of the *SAT1* cassette to generate RSY542 and CAY4160, and transformed with the *STE12* deletion construct to generate RSY543 and RSY610, RSY611, RSY612, respectively. These strains were incubated on SC-Maltose to excise *SAT1* to generate RSY564, CAY4240, CAY4241, and CAY4242.

Haploid *ste12* strains RSY539, RSY535, RSY544, and RSY545 were generated by incubating RSY541 (*STE12/ste12* heterozygote) on PDA medium for 3 days to generate haploid progeny. The *MTL* of these progeny was checked by PCR using oligonucleotides RS66/67 and RS68/69. PCR using primers RS399/RS400 was used to verify the absence of *STE12*.

The *C. lusitaniae STE12* gene was reintegrated into a *ste12 /ste12* strain (RSY564). The *STE12* ORF, together with ~1 kb of the promoter, was PCR amplified using oligonucleotides RS401/RS402. pSFS2a and the *STE12* PCR product were digested with *KpnI* and *ApaI* and ligated together. The resulting construct was linearized using *BmgBI* and transformed into RSY564 to generate complemented strains RSY601, RSY602, and RSY603. Accurate integration of the construct was determined by PCR using oligonucleotides RS403/RS345.

Construction of *K. lactis* strains

To obtain diploid *K. lactis* strains, CAY571 and CAY572 were mated on malt medium at 30°C and selected on medium lacking tryptophan and uracil to generate RSY467, RSY468, RSY469, RSY470, and RSY478. *K. lactis* mutants were generated using an electroporation protocol previously described³⁷. To make gene deletion cassettes, *STE12* 5' and 3' homologous flanks were generated by PCR of genomic DNA using oligonucleotides BL1581/BL1568 and BL1569/BL1582 respectively. Nourseothricin and Kanamycin resistant genes were amplified by PCR using plasmids pKANmx4 and pNATmx4⁴² with primers BL1313 and BL1414. Resistance genes were fused to target gene-flanking regions by fusion PCR⁴³ using oligonucleotides BL1581/BL1582. This created two linear DNA constructs for transformation, *STE12-NAT* and *STE12-KAN*. *STE12* double mutants were generated by two sequential rounds of transformation. RSY478 was first transformed with the *STE12-KAN* cassette to obtain RSY551 and RSY555. Accurate integration was verified by PCR across 5' and 3' junctions using oligonucleotides BL1500/BL1329 and BL1501/BL1330. RSY551 and RSY555 strains were transformed with the *STE12-NAT* construct to obtain *ste12 /ste12* strains RSY571/RSY572 and RSY574, respectively. Loss of the *STE12* ORF was verified by PCR (BL1498/BL1499). Haploid *K. lactis STE12* mutants were

generated by transforming CAY571 with the *STE12-NAT1* cassette to generate RSY567 and RSY568. CAY572 was transformed with *STE12-KAN* to generate RSY550 and with *STE12-NAT* to generate RSY570.

Construction of *P. pastoris* and *Y. lipolytica* strains

To delete the *STE12* gene in *Pichia pastoris*, 5' and 3' flanks of the gene were amplified by PCR using oligonucleotides 2357/2358 and 2359/2360. *HYG* or *NAT1* selection markers were PCR amplified using oligonucleotides BL1309/BL1310 from plasmids pNatMX4 and pHYGMX4. The *KAN* marker was PCR amplified from plasmid pKANB⁴⁴ using oligonucleotides 2365/2366. *STE12* flanks and selection markers were joined by fusion PCR using oligonucleotides 2357/2360. PCR constructs were then transformed into *P. pastoris* strains JC304 and JC306 using an established protocol³⁴.

To delete the *STE12* gene in *Yarrowia lipolytica*, the *STE12* ORF and flanking regions were first amplified by PCR using oligonucleotides BL2618/BL2619 and cloned into pCR-Blunt II-TOPO (Invitrogen) to generate pRB339. The *LEU2* gene was also PCR amplified from *Y. lipolytica* using oligonucleotides BL2620/BL2621 and cloned into pCR-BluntII-TOPO. *LEU2* was then excised from this vector using *Bam*HI/*Kpn*I and used to replace the *STE12* ORF in pRB340. A cassette was released from this vector using *Hind*III/*Eco*RV and used to transform *Y. lipolytica* to delete the *STE12* gene. The *URA3* gene was also amplified from vector pINA156 (gift from Carmen Lisset-Flores Mauriz, Instituto de Investigaciones Biomédicas Alberto Sols CSIC-UAM, Madrid) using primers BL2622/BL2483 and cloned into pSC-B-amp/kan (Agilent). *URA3* was excised from this vector and used to replace *STE12* in vector pRB341. Subsequently, a cassette was released from this vector using *Hind*III/*Eco*RV and transformed into *Y. lipolytica* to delete *STE12*. Transformations in *Y. lipolytica* were achieved using the lithium acetate method of Barth and Gaillardin⁴⁵.

Construction of *S. cerevisiae* strains

Diploid *S. cerevisiae* strains were generated by mating CAY4584 and CAY4585 on YPD medium for 24 h, then selecting for diploid products on SCD medium lacking tryptophan and adenine. The resulting mating product, CAY4595, was verified as being diploid by its ability to sporulate and PCR of the *MAT* locus using primers 2461/2562 (*MAT* α 1) and 2565/2566 (*MAT* α 1). Subsequent transformations were performed as described⁴⁶. To delete the *STE12* gene, oligonucleotides BL2468/BL2469 were used to PCR amplify selection markers from pNATMX4 and pKANMX4 and contained sequences that were complementary to the 5' and 3' regions of the *STE12* ORF. Transformation using a *NATMX4-STE12* PCR construct generated strain CAY4770, which was PCR checked using primers BL1329/BL2470 and BL1330/BL2471. CAY4770 was transformed with a *KANMX4-STE12* PCR construct to generate CAY4808, a *ste12* /*ste12* deletion mutant. Loss of the ORF was confirmed by PCR with primers BL2472/BL2473.

Microarray Design

C. lusitaniae genomic sequences were downloaded from the Broad Institute (<http://www.broadinstitute.org>) to design a custom 8 × 15 K microarray using Agilent eArray. Each array had a minimum of two independent 60-mer oligonucleotides designed against the

5,941 open reading frames encoded by the *C. lusitaniae* genome, resulting in a total of 11,882 unique oligonucleotides on each microarray.

Cell preparation for microarray analysis

To analyze meiosis, diploid *C. lusitaniae* strains were grown on PDA (meiosis-inducing) or YPD (non-inducing) medium. Cells from wild type strain RSY432 were removed after 0.5, 2, 4, 8, 12, 18, 24 and 30 h on solid PDA medium and flash frozen in liquid nitrogen. For *ime2 /ime2* and *ste12 /ste12* profiling, cells from strain RSY428 and CAY4240 were incubated on solid PDA medium for 0, 12, 18, and 24 h and flash frozen. RSY432 cell aliquots were collected after 2 h incubation on YPD and used as a reference for all meiosis-profiling experiments. For mating profiles, 6.6×10^7 RSY284 (a) and RSY411 (α) cells were co-incubated on PDA medium for 0, 4 and 12 h and frozen. For comparison, 6.6×10^7 RSY410 (a) and RSY406 (α) cells were co-incubated on PDA medium for 4 h to profile *ime2* mating expression patterns. RSY284 a cells incubated on YPD for 4 h were used as a reference sample for mating profiles.

Microarray analysis

RNA was isolated from cells using the Ribopure yeast RNA extraction kit (Ambion). RNA was treated with turbo DNAase (Ambion) and evaluated for quality and purity using an Agilent bioanalyzer. Approximately 10 μg of total RNA was used for each cDNA synthesis reaction. Random oligonucleotides (pdN₉) as well as dT₁₉ oligos were annealed to total RNA. cDNA was synthesized using Superscript III reverse transcriptase (Invitrogen) in reaction mixes containing 0.25 mM DTT and 0.5 mM total deoxynucleotide phosphates added in a ratio of 3:2 aminoallyl-dUTP/dNTPs. cDNA reactions were stopped after 3 h incubation and subject to 0.3 M NaOH/0.3 M EDTA hydrolysis at pH 7. Single-stranded cDNA was purified and concentrated using a Zymo Cleaner and Concentrator kit (25 μg capacity columns). cDNA concentration was determined and each sample separated into 2 μg aliquots, speed vacuumed, and resuspended in 9 μL of water.

cDNA was labeled by incubation with Cy3 or Cy5 dyes in DMSO and 1 M sodium bicarbonate, and concentrated using a Zymo Cleaner and Concentrator spin column kit. Final cDNA concentration and dye-incorporation were determined by nanodrop using the “microarray” setting (Nanodrop 2000c, Thermo Scientific). Approximately 300 ng of labeled experimental cDNA was pooled with an equal amount of reference cDNA to a final volume of 25 μl. Pooled cDNA was denatured at 95°C, mixed with 2x GE Hybridization buffer (HI-RPM buffer, Agilent) and applied to the array. Arrays were incubated for 18 h at 65°C and sequentially washed in Agilent Wash Buffer I, Agilent Wash Buffer II, acetonitrile (Sigma-Aldrich) and Agilent drying and stabilization buffer.

Slides were scanned on an Axon 4000B slide scanner (GenePix) and fluorescence quantified using GENE Pix Pro software. Data was normalized using Goulphar (<http://transcriptome.ens.fr/goulphar>)³⁸. Normalized gene expression data was averaged for all array replicates and used to generate heatmaps. Pair wise average linkage clustering was performed by Cluster (<http://bonsai.hgc.jp/~mdehoon/software/cluster/software.htm>) and heatmaps visualized using treeview (<http://jtreeview.sourceforge.net/>)^{39,40}. All microarray

data has been deposited into the NCBI Gene Expression Omnibus (GEO) portal under accession number GSE51794.

Genetic assays for *C. lusitaniae* mating, meiosis, and recombination

Throughout this study we utilize genetic crosses between *C. lusitaniae* strains RSY284 (*MTLa*) and RSY411 (*MTLa*). These strains carry different auxotrophic markers that allows for selection of mating products. The diploid product of mating, RSY432, is heterozygous for the cycloheximide recessive genetic marker (chx^R). This allows for selection of haploid (meiotic) progeny by growth on cycloheximide, whereas diploid parents (chx^R/chx^S) do not grow on this medium (see Extended Data Fig. 5). The formation of haploid meiotic progeny was also defined by determining the fraction of *ade*- colonies due to loss of the *ADE2* gene on chromosome 5.

Mating Assays

C. lusitaniae strains were incubated in liquid YPD medium overnight and washed in water. Aliquots of 2×10^7 cells of each mating type were mixed and cultured on PDA medium at 24°C for 1-5 days. Aliquots of cells were removed and plated for selection of parents as well as diploid products. Percentage of diploid formation = $100 \times (\# \text{ of colonies on double selection medium} / \# \text{ minimal parents on single selection medium})$. Double selection medium was SCD –uracil –arginine, while single selection medium was SCD – arginine and SCD – uracil. Subsets of cells were screened for ploidy by flow cytometry and *MTLa*/ α alleles were verified by PCR using oligonucleotides RS68/RS69 and R66/RS67. Experiments were repeated in three biological replicates for *ste12* assays and four biological replicates for *ime2* assays. Wildtype crosses: RSY284 x RSY411, *ime2* cross: RSY406 x RSY410. *IME2* complemented cross: RSY406 x CAY5022. *ste12* cross, RSY539 x RSY545.

K. lactis strains were incubated in liquid YPD medium overnight. Aliquots of 2×10^7 cells of each mating type were mixed and cultured on malt medium at 30°C for 3 days. Aliquots of cells were removed and plated for selection of parents as well as diploid products. Diploid formation was quantified as for *C. lusitaniae*. Diploid selection media was SC –tryptophan – adenine, while single selection media was SC- tryptophan and SC – adenine. Experiments were repeated in two biological replicates with four independent *ste12* strains. WT crosses: CAY571 x CAY572. *ste12* crosses: RSY550 x RSY567, RSY570 x RSY568.

P. pastoris strains were incubated in YPD medium overnight. Aliquots of 2×10^7 cells of each mating type were washed, mixed, and cultured on sodium acetate medium at 24°C for 5 days. Cells were removed and plated for selection of parents as well as diploid products. Diploid formation was quantified as for *C. lusitaniae*. Diploid selection medium was SC- histidine-arginine, while single selection media was SC-histidine and SC –arginine. Experiments were repeated in three biological replicates. WT cross: JC304 x JC306. WT x *ste12* crosses: RBY4440 x JC306, RBY4441 x JC306.

Meiosis Assays

For *C. lusitaniae* assays, strains were incubated in YPD overnight, washed in water, and 6×10^7 cells spread onto PDA plates. Cells were incubated at 24°C and then plated onto YPD

and haploid selection media (YPD+ cycloheximide). Sporulation percentage was calculated as $100 \times (\text{cells on haploid selection media} \times 2) / (\text{cells on YPD})$. Experiments were repeated in three biological replicates. Wildtype sporulation: RSY432. *ime2 /ime2* sporulation: #1, RSY427, #2, RSY248, #3, RSY429. *ste12 /ste12* sporulation: RSY543 (Fig. 3) and CAY4240 (Extended Data Fig. 5c).

For *K. lactis* assays, diploid strains were incubated on malt medium at 30°C for 3 days to induce meiosis. Cells were removed and approximately 200 cells plated onto YPD. Sporulation percentage was calculated as $100 \times (\text{ade- cells} \times 2) / (\text{total cells})$. Meiosis assays were performed in two biological replicates with three independent *ste12 /ste12* mutants. For *S. cerevisiae* meiosis assays, strains were incubated in YPA medium (2% peptone, 1% yeast extract, 1% KOAc) at 30°C to an OD₆₀₀ of 1.5-2.5. Cells were washed and resuspended in sporulation medium (1% KOAc, 0.02% raffinose) to an OD₆₀₀ of 1.5. Cells were incubated in sporulation medium at 30°C for 24 hours and then plated onto YPD. Sporulation was calculated as $100 \times (\text{ade- cells} \times 2) / (\text{total cells})$. The experiment was performed in three biological replicates. For *P. pastoris* meiosis assays, diploid cells were incubated on sodium acetate medium for 6 days. Cells were recovered and approximately 200 cells plated onto YPD medium. The sporulation percentage was defined as $100 \times (\text{ade-cells} \times 2) / (\text{total cells})$. The experiment was performed in four biological replicates. To induce meiosis in *Y. lipolytica*, cells were grown on V8 medium at 24°C for 7 days. Meiotic spores were subsequently identified by staining cells with a 5% solution of malachite green⁴¹.

Statistical Analysis of Mating and Meiosis Data

Analysis of *C. lusitaniae* *IME2* meiosis data was performed on log-transformed data. Data were normally distributed ($p > 0.05$, Anderson Darling test) and homoscedastic ($p > 0.05$, Levene's test for homogeneity of variance), and one way ANOVA was performed. In *ime2* mating and *ste12* mating experiments, the data was not normally distributed or displayed heteroscedasticity, and a Kruskal-Wallis test was performed to compare across wildtype, unilateral, and bilateral crosses. In *ste12 /ste12* meiosis experiments, pairwise comparisons were made between wildtype and *ste12 /ste12* mutants using an unequal variance t-test.

Pheromone Detection Assay

A wildtype *C. lusitaniae* diploid strain and *C. albicans* CAY3705 strain were cultured in SCD medium at 24°C overnight. CAY3705 contains a chimeric *STE2* pheromone receptor; the majority of the receptor sequence is derived from *C. lusitaniae* Ste2, while the intracellular C-terminal tail is from *C. albicans* Ste2. Previous studies have shown that *C. albicans* cells expressing the chimeric receptor can respond to synthetic *C. lusitaniae* α pheromone²¹. CAY3705 is also expressing a fluorescent nuclear reporter (a histone HTB-YFP fusion protein). Cells were washed in water and 4×10^7 *C. lusitaniae* cells mixed with 0.4×10^7 CAY3705 cells and plated onto PDA plates at 24°C. Cells were removed from PDA plates after 14-18 h incubation and imaged using a Zeiss Observer Z1 microscope.

Microscopy

Differential interference contrast (DIC) and fluorescent images of cells were captured using a Zeiss Inverted Microscope (Axio Observer. Z1) fitted with an AxioCam HR. Images were processed with AxioVision Rel. 4.8 (Zeiss, Germany). For analysis of *C. lusitaniae* cell morphology during meiosis, diploid a/α cells were incubated on PDA medium at 24°C and samples taken at the indicated time points in Extended Data Fig. 2c and examined microscopically. At least 300 cells per strain were examined for a change in morphology (defined as polarized growth of the cell) or for spore formation.

Defining *C. lusitaniae* Gene Expression Changes During Meiosis

Fold induction of *C. lusitaniae* meiotic genes demonstrating expression patterns characteristic of early, middle and late meiosis were determined by evaluating microarray data. Genes were characterized as being induced during meiosis if they exhibited >3-fold induction after 12, 18, or 24 h on PDA and also demonstrated < 3-fold induction in haploid a and α cells incubated on PDA medium for 30 min, 2 h, or 24 h. This analysis generated a set of 618 genes. The resulting list of genes was then compared to genes induced during *ime2* / *ime2* meiosis data to determine the number of meiosis-specific genes dependent on Ime2 (Extended Data Fig. 3e). This same set of 618 genes was used to compare to gene induction during meiosis of *ste12* / *ste12* mutant cells.

Analyzing MAPK gene expression during *C. lusitaniae* meiosis

Average fold gene induction was calculated by averaging expression changes of *S. cerevisiae* MAPK genes (*STE20*, *STE11*, *STE7*, *FUS3*, *STE12*, *STE2*, *STE3*, *GPA1*, *STE4*, *STE18*, *MFALPHA* and *KSS1*) or their *C. lusitaniae* orthologs during meiosis. *S. cerevisiae* gene expression data was from Roberts *et al.*³⁰ and was enhanced 3 fold to be comparable to expression changes in *C. lusitaniae* genes.

RT-PCR

WT strains RSY411 and RSY284 were mated on PDA at 24°C. Aliquots of mating mixes were snap frozen after 0 min, 30 min, 2 h, 4 h and 24 h of co-incubation. pdN9 was annealed to 2 µg of RNA extracted from the mating mixes. First strand cDNA was synthesis was performed with GoScript reverse transcriptase (Promega). 75 ng of the resulting cDNA was PCR amplified for *IME2* and *ACT1* expression using oligonucleotides RSY183/RSY184 and RS333/RS334.

Supplementary Material

Refer to Web version on PubMed Central for supplementary material.

Acknowledgements

We thank Joseph Heitman, Carmen Lisset-Flores Mauriz, Thierry Noel, Neil Hunter, and Jennifer Reedy for gifts of strains and plasmids, and Shail Kabrawala and Nayimisha Balmuri for help with strain construction. We also thank Trevor Sorrells, Liam Holt, and members of the Johnson and Bennett labs for comments on the paper, and Stephen Jones for help with statistical analysis. This work was supported by National Science Foundation Grant MCB1021120 (to R.J.B.), by National Institutes of Health R01 Grant AI081704 (to R.J.B.), by T32GM007601 (to

C.M.S.), by F31AI075607 (To R.K.S.), and by an Investigator in the Pathogenesis of Infectious Disease Award from the Burroughs Wellcome Fund (to R.J.B.).

References

1. van Werven FJ, Amon A. Regulation of entry into gametogenesis. *Philos Trans R Soc Lond B BiolSci.* 2011; 366:3521–3531. doi:366/1584/3521[pii]10.1098/rstb.2011.0081. [PubMed: 22084379]
2. Wong Sak Hoi J, Dumas B. Ste12 and Ste12-like proteins, fungal transcription factors regulating development and pathogenicity. *Eukaryot Cell.* 2010; 9:480–485. doi:EC.00333-09 [pii]10.1128/EC.00333-09. [PubMed: 20139240]
3. Irniger S. The Ime2 protein kinase family in fungi: more duties than just meiosis. *MolMicrobiol.* 2011; 80:1–13. doi:10.1111/j.1365-2958.2011.07575.x.
4. Yoshida M, et al. Initiation of meiosis and sporulation in *Saccharomyces cerevisiae* requires a novel protein kinase homologue. *Mol Gen Genet.* 1990; 221:176–186. [PubMed: 2196430]
5. Dolan JW, Kirkman C, Fields S. The yeast STE12 protein binds to the DNA sequence mediating pheromone induction. *Proc Natl Acad Sci U S A.* 1989; 86:57035707.
6. Errede B, Ammerer G. STE12, a protein involved in cell-type-specific transcription and signal transduction in yeast, is part of protein-DNA complexes. *Genes Dev.* 1989; 3:1349–1361. [PubMed: 2558054]
7. Souza CA, Silva CC, Ferreira AV. Sex in fungi: lessons of gene regulation. *Genetics and Molecular Research : GMR.* 2003; 2:136–147. [PubMed: 12917810]
8. Govin J, Berger SL. Genome reprogramming during sporulation. *IntJ Dev Biol.* 2009; 53:425–432. doi:082687jg [pii]10.1387/ijdb.082687jg. [PubMed: 19412896]
9. Butler G, et al. Evolution of pathogenicity and sexual reproduction in eight *Candida* genomes. *Nature.* 2009; 459:657–662. doi:nature08064[pri]10.1038/nature08064. [PubMed: 19465905]
10. Reedy JL, Floyd AM, Heitman J. Mechanistic plasticity of sexual reproduction and meiosis in the *Candida* pathogenic species complex. *Curr Biol.* 2009; 19:891–899. doi:S0960-9822(09)01057-4 [pii]10.1016/j.cub.2009.04.058. [PubMed: 19446455]
11. Gargeya IB, Pruitt WR, Simmons RB, Meyer SA, Ahearn DG. Occurrence of *Clavispora lusitaniae*, the teleomorph of *Candida lusitaniae*, among clinical isolates. *J Clin Microbiol.* 1990; 28:2224–2227. [PubMed: 2229346]
12. Lengeler KB, et al. Signal transduction cascades regulating fungal development and virulence. *Microbiol Mol Biol Rev.* 2000; 64:746–785. [PubMed: 11104818]
13. Butler G. Fungal sex and pathogenesis. *Clin Microbiol Rev.* 2010; 23:140–159. doi:23/1/140 [pii]10.1128/CMR.00053-09. [PubMed: 20065328]
14. Keeney, S. *Recombination and Meiosis Vol. 2 Genome Dynamics and Stability.* Lankenau, D., editor. Springer; Berlin/Heidelberg: 2007.
15. Klein F, et al. A central role for cohesins in sister chromatid cohesion, formation of axial elements, and recombination during yeast meiosis. *Cell.* 1999; 98:91–103. doi:S0092-8674(00)80609-1 [pii]10.1016/S0092-8674(00)80609-1. [PubMed: 10412984]
16. Smith HE, Mitchell AP. A transcriptional cascade governs entry into meiosis in *Saccharomyces cerevisiae*. *Mol Cell Biol.* 1989; 9:2142–2152. [PubMed: 2664470]
17. Chu S, et al. The transcriptional program of sporulation in budding yeast. *Science.* 1998; 282:699–705. [PubMed: 9784122]
18. Guttmann-Raviv N, Martin S, Kassir Y. Ime2, a meiosis-specific kinase in yeast, is required for destabilization of its transcriptional activator, Ime1. *Mol Cell Biol.* 2002; 22:2047–2056. [PubMed: 11884593]
19. Holt LJ, Hutti JE, Cantley LC, Morgan DO. Evolution of Ime2 phosphorylation sites on Cdk1 substrates provides a mechanism to limit the effects of the phosphatase Cdc14 in meiosis. *Mol Cell.* 2007; 25:689–702. doi:S1097-2765(07)00112-8 [pii]10.1016/j.molcel.2007.02.012. [PubMed: 17349956]

20. Sopko R, Raithatha S, Stuart D. Phosphorylation and maximal activity of *Saccharomyces cerevisiae* meiosis-specific transcription factor Ndt80 is dependent on Ime2. *Mol Cell Biol.* 2002; 22:7024–7040. [PubMed: 12242283]
21. Lin CH, Choi A, Bennett RJ. Defining pheromone-receptor signaling in *Candida albicans* and related asexual *Candida* species. *Mol Biol Cell.* 2011; 22:49184930. doi:mbc.E11-09-0749 [pii]10.1091/mbc.E11-09-0749.
22. Young LY, Lorenz MC, Heitman J. A STE12 homolog is required for mating but dispensable for filamentation in *Candida lusitanae*. *Genetics.* 2000; 155:17–29. [PubMed: 10790381]
23. Sipiczki M. Where does fission yeast sit on the tree of life? *Genome Biol.* 2000; 1:1011.1011–1011.1014.
24. Sugimoto A, Iino Y, Maeda T, Watanabe Y, Yamamoto M. *Schizosaccharomyces pombe* ste11+ encodes a transcription factor with an HMG motif that is a critical regulator of sexual development. *Genes Dev.* 1991; 5:1990–1999. [PubMed: 1657709]
25. Kjaerulff S, Lautrup-Larsen I, Truelsen S, Pedersen M, Nielsen O. Constitutive activation of the fission yeast pheromone-responsive pathway induces ectopic meiosis and reveals Ste11 as a mitogen-activated protein kinase target. *Mol Cell Biol.* 2005; 25:2045–2059. [PubMed: 15713656]
26. Herskowitz I. A regulatory hierarchy for cell specialization in yeast. *Nature.* 1989; 342:749–757. doi:10.1038/342749a0. [PubMed: 2513489]
27. Booth LN, Tuch BB, Johnson AD. Intercalation of a new tier of transcription regulation into an ancient circuit. *Nature.* 2010; 468:959–963. doi:nature09560 [pii]10.1038/nature09560. [PubMed: 21164485]
28. Otto SP. The evolutionary consequences of polyploidy. *Cell.* 2007; 131:452–462. [PubMed: 17981114]
29. Otto SP, Gerstein AC. The evolution of haploidy and diploidy. *Curr Biol.* 2008; 18:R1121–1124. doi:S0960-9822(08)01268-2 [pii]10.1016/j.cub.2008.09.039. [PubMed: 19108763]
30. Roberts CJ, et al. Signaling and circuitry of multiple MAPK pathways revealed by a matrix of global gene expression profiles. *Science.* 2000; 287:873–880. [PubMed: 10657304]
31. Guthrie, C.; Fink, GR. *Guide to Yeast Genetics and Molecular Biology.* Academic Press; San Diego: 1991.
32. Gargeya IB, Pruitt WR, Simmons RB, Meyer SA, Ahearn DG. Occurrence of *Clavispora lusitanae*, the teleomorph of *Candida lusitanae*, among clinical isolates. *J. Clin. Microbiol.* 1990; 28:2224–2227. [PubMed: 2229346]
33. Reuß O, Vik A, Kolter R, Morschhauser J. The SAT1 flipper, an optimized tool for gene disruption in *Candida albicans*. *Gene.* 2004; 341:119–127. [PubMed: 15474295]
34. Cregg, JM., et al. Expression in the Yeast *Pichia pastoris*, in *Methods Enzymology.* Burgess, RR.; Deutscher, MP., editors. Vol. 463. Elsevier; 2009. p. 169-189.
35. El-Kirat-Chatel S, Dementhon K, Noël T. A two-step cloning-free PCR-based method for the deletion of genes in the opportunistic pathogenic yeast *Candida lusitanae*. *Yeast.* 2011; 28:321–330. [PubMed: 21456057]
36. François F, Chapeland-Leclerc F, Villard J, Noël T. Development of an integrative transformation system for the opportunistic pathogenic yeast *Candida lusitanae* using URA3 as a selection marker. *Yeast.* 2004; 21:95–106. [PubMed: 14755635]
37. Kooistra R, Hooykaas PJ, Steensma HY. Efficient gene targeting in *Kluyveromyces lactis*. *Yeast.* 2004; 21:781–792. [PubMed: 15282801]
38. Lemoine S, Combes F, Servant N, Le Crom S. Goulphar: rapid access and expertise for standard two-color microarray normalization methods. *BMC bioinformatics.* 2006; 7:467. [PubMed: 17059595]
39. Saldanha AJ. Java Treeview—extensible visualization of microarray data. *Bioinformatics.* 2004; 20:3246–3248. [PubMed: 15180930]
40. de Hoon MJL, Imoto S, Nolan J, Miyano S. Open source clustering software. *Bioinformatics.* 2004; 20:1453–1454. [PubMed: 14871861]
41. Flores CL, Gancedo C, Petit T. Disruption of *Yarrowia lipolytica* TPS1 gene encoding trehalose-6-P synthase does not affect growth in glucose but impairs growth at high temperature. *PLoS One.* 2011; 6:e23695. [PubMed: 21931609]

42. Wach A, Brachat A, Pohlmann R, Philippsen P. Dominant marker vectors for selecting yeast mating products. *Yeast*. 2008; 52:595–599.
43. Noble SM, Johnson AD. Strains and strategies for large-scale gene deletion studies of the diploid human fungal pathogen *Candida albicans*. *Eukaryot Cell*. 2005; 4:298–309. [PubMed: 15701792]
44. Lin-Cereghino J, et al. Direct selection of *Pichia pastoris* expression strains using new G418 resistance vectors. *Yeast*. 2008; 25:293–299. [PubMed: 18327886]
45. Barth G, Gaillardin C. Physiology and genetics of the dimorphic fungus *Yarrowia lipolytica*. *FEMS microbiology reviews*. 1997; 19:219–237. [PubMed: 9167256]
46. Schiestl RH, et al. *Methods: A Companion to Meth. Enzy.* 1993; 5:79–85.

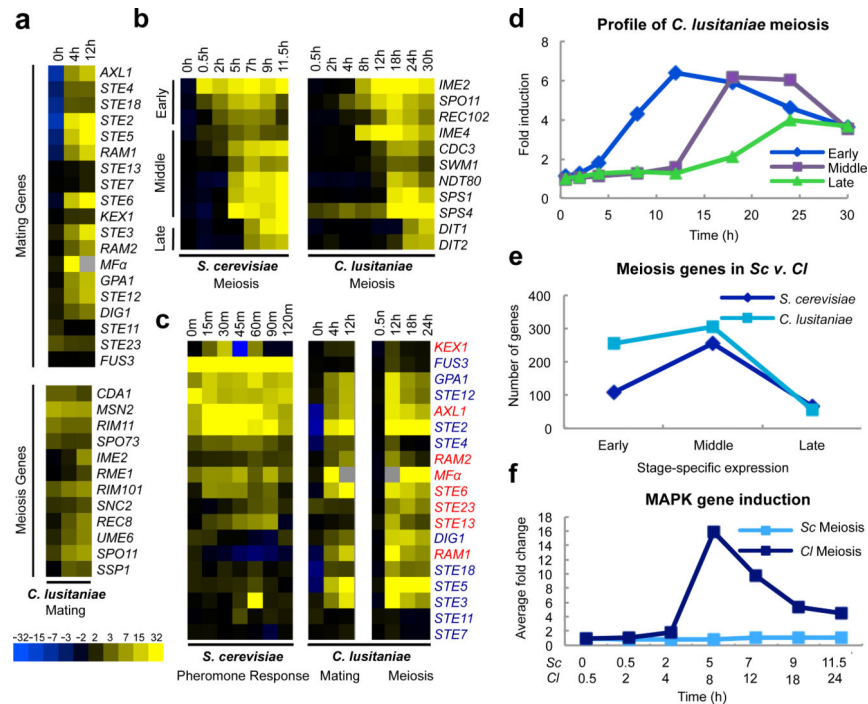


Figure 1. Transcriptional profiling of mating and meiosis in *C. lusitaniae*. **a**, Profiling of *C. lusitaniae* mating. Top panel, induction of *C. lusitaniae* pheromone-signaling genes. Bottom panel, induction of genes characteristic of the meiotic program in *S. cerevisiae*. **b**, Stage-specific meiotic gene expression in *S. cerevisiae* and *C. lusitaniae*. Early, Middle, and Late meiosis genes in *C. lusitaniae* are defined as those >3 fold induced after 12, 18, and 24 h, respectively. **c**, Expression of MAPK pathway genes (blue text) and pheromone-processing genes (red text) during *C. lusitaniae* mating and meiosis. Expression changes for *S. cerevisiae* genes³⁰ were enhanced 3-fold to be comparable to expression changes in *C. lusitaniae* genes. **d**, Average fold induction of early, middle, and late meiosis genes in *C. lusitaniae*. **e**, Comparison of meiosis gene expression changes in *C. lusitaniae* and *S. cerevisiae*. **f**, Fold induction of MAPK pathway genes during meiosis in *C. lusitaniae* and *S. cerevisiae*.

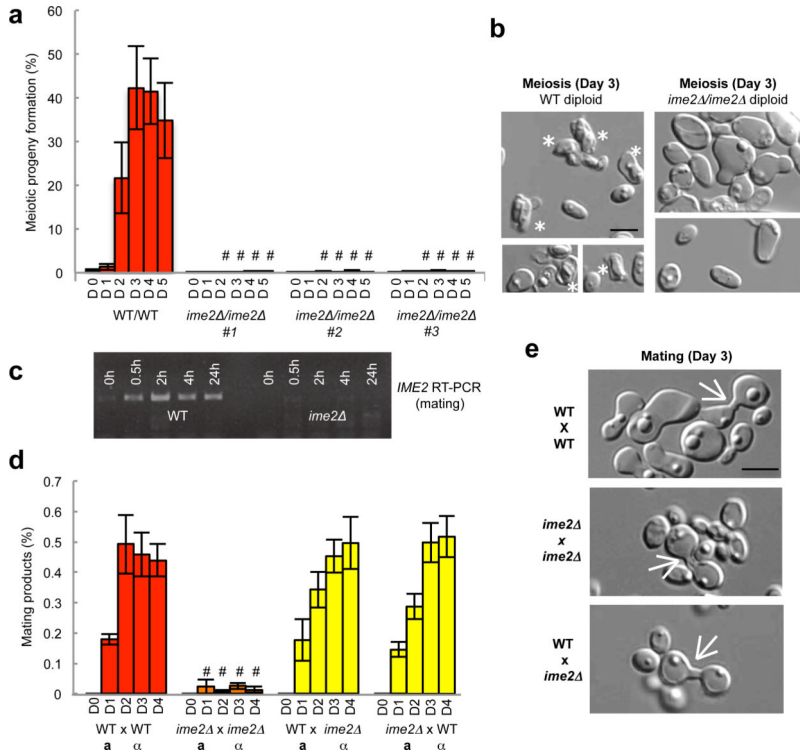


Figure 2. *IME2* is required for both mating and meiosis in *C. lusitaniae*. **a**, Deletion of *IME2* blocks meiosis in *C. lusitaniae* (5-day time course, D1-D5). # represents $p < 0.01$, one way ANOVA, $n=3$. **b**, Wildtype diploid cells generate dyad spores (asterisks) after 3 days on PDA medium, whereas *ime2* /*ime2* diploids do not sporulate, $n=3$. **c**, RT-PCR data demonstrates induction of *IME2* during *C. lusitaniae* mating, $n=3$. **d**, Loss of *IME2* in both α and a cells leads to decreased mating (4 day time course, D1-D4). “#” represents $P < 0.05$, Kruskal Wallis, $n=4$. **e**, *ime2* mutants generate mating zygotes, indicating the block to mating occurs post-cell fusion, $n=4$. Scale bars, 5 μm . Data represented as mean \pm s.e.m.

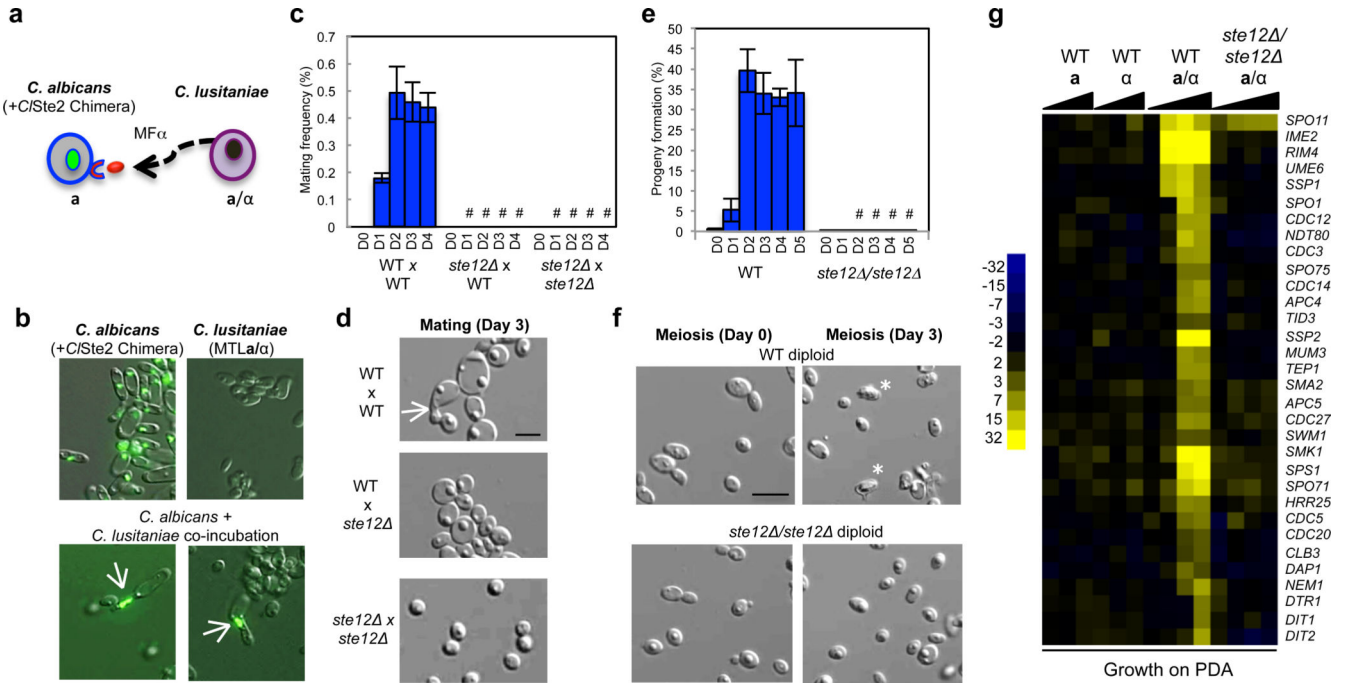


Figure 3. *STE12* is essential for both mating and meiosis in *C. lusitaniae*. **a**, Schematic of assay to detect pheromone secretion from *C. lusitaniae* cells. *C. lusitaniae* a/α cells were co-incubated with GFP-labeled *C. albicans* a cells expressing the *C. lusitaniae* α pheromone receptor. **b**, *C. albicans* cells generate polarized mating projections (arrows) in response to *C. lusitaniae* pheromone, demonstrating that *C. lusitaniae* cells actively secrete pheromone during meiosis, n=2. **c**, Deletion of *STE12* abolishes mating in *C. lusitaniae* (4 day time course, D1-D4). “#” represents P < 0.05, Kruskal Wallis, n=3. **d**, Mating occurs between wildtype *C. lusitaniae* cells (arrow) but not between *ste12* mutant cells, n=3. **e**, Loss of *STE12* inhibited the formation of meiotic haploid progeny (4 day time course, D1-D4). “#” represents P < 0.05, unequal variance t test, n=3. **f**, Absence of meiotic spores in *C. lusitaniae* cells lacking *STE12*, n=5. **g**, Gene expression changes when *C. lusitaniae* haploid, diploid, or *ste12* /*ste12* strains are incubated on PDA medium. Deletion of *STE12* abolished most meiosis-specific gene expression changes. Where appropriate, scale bars, 5 μm; data represented as mean +/- s.em.

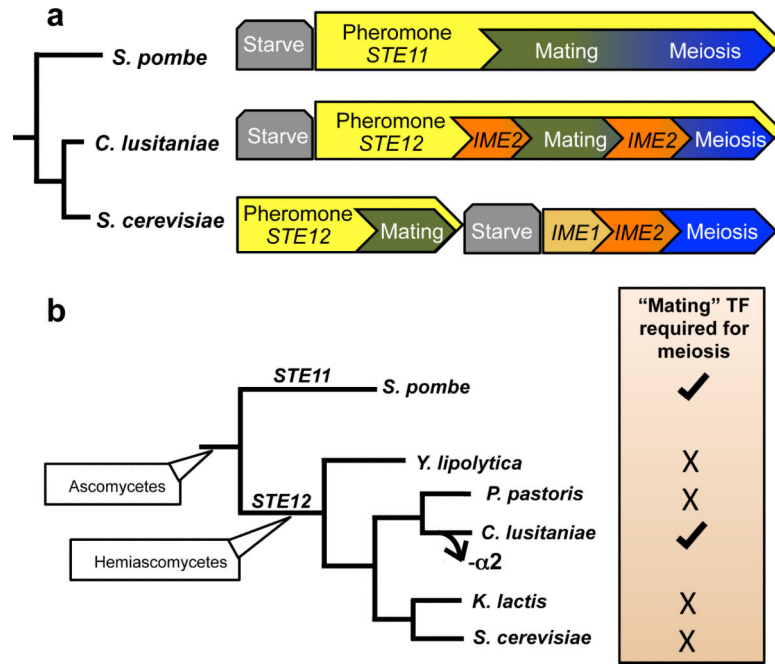
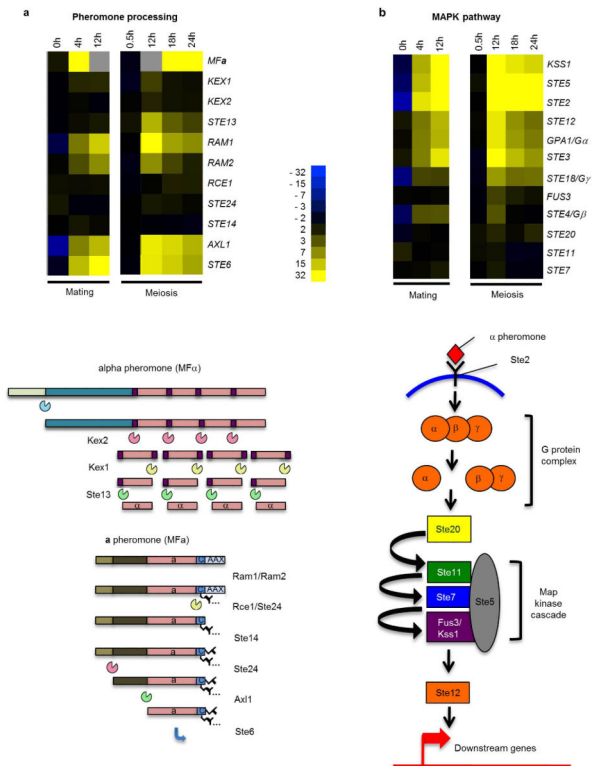
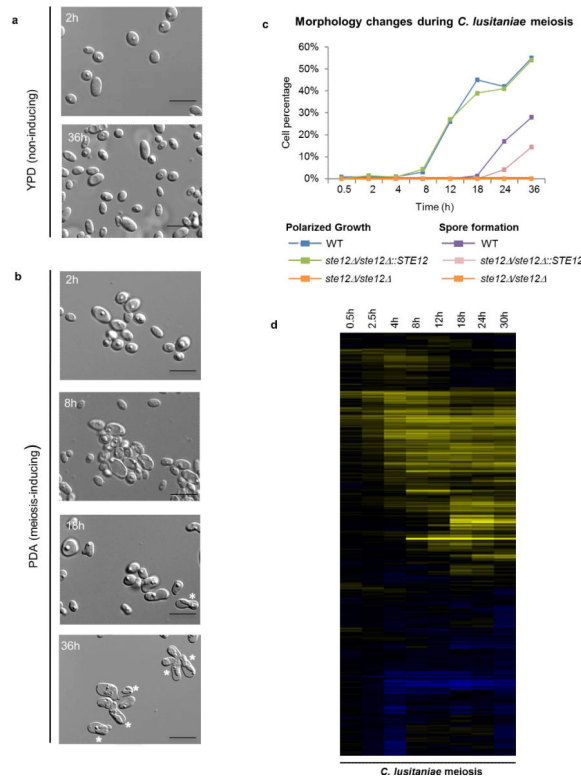


Figure 4.

Sexual regulation in yeast. **a**, Model comparing the sexual lifecycles of *S. cerevisiae*, *C. lusitaniae*, and *S. pombe*. The diploid species *S. cerevisiae* exhibits distinct regulation of mating and meiosis; MAPK signaling via Ste12 regulates mating, while Ime1 regulates meiosis. In contrast, *S. pombe* exhibits integrated control of its sexual cycle; MAPK signaling and Ste11 regulate entry into both mating and meiosis. *C. lusitaniae* exhibits similar control over its sexual cycle to that in *S. pombe*. In particular, *C. lusitaniae* mating and meiosis are highly coupled, and both are regulated by the transcription factor Ste12. **b**, *C. lusitaniae* is the only hemiascomycete tested that requires *STE12* to undergo meiosis. Loss of the *MTLα2* transcription factor specifically in the *C. lusitaniae* lineage could have been a key step during evolution of this regulatory control, as it would permit expression of ‘haploid-specific genes’ (including MAPK genes) in diploid cells.

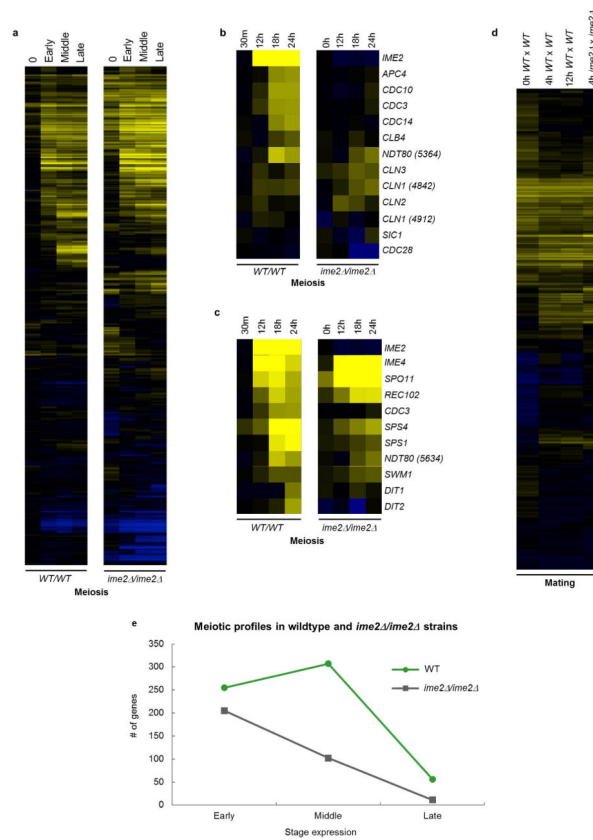


Extended Data Figure 1. Schematic showing induction of (a) pheromone-processing genes and (b) pheromone MAPK genes during both mating and meiosis in *C. lusitaniae*
 Expression changes highlight genes induced during co-incubation of **a** and α cells on PDA medium (mating), as well as during growth of diploid **a**/ α cells on PDA medium (induces meiosis and sporulation). In contrast, these genes are mating-specific in the related yeast *S. cerevisiae*.



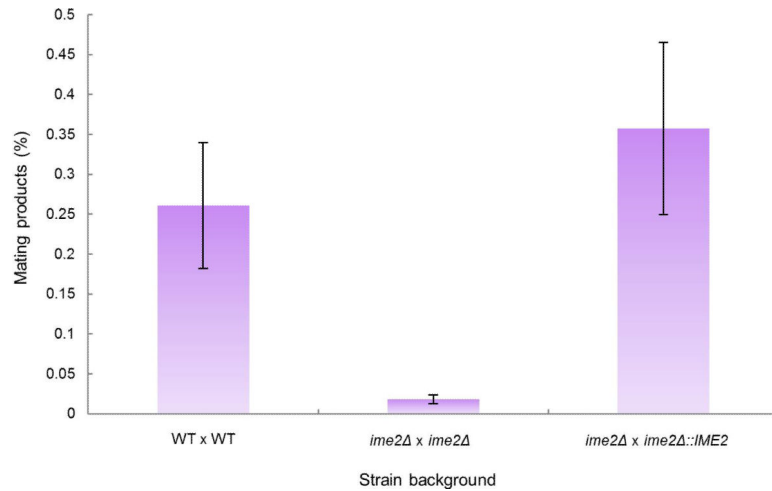
Extended Data Figure 2. Temporal analysis of meiosis in *C. lusitaniae*

a, *C. lusitaniae* a/a cells divide as stable diploid cells on YPD medium. $n=3$. **b**, On PDA medium, a/a cells are induced to enter meiosis and dyad spores (asterisks) begin to appear at 18 h. $n=3$. **c**, Time course of meiosis in wildtype, *ste12* $\Delta/ste12$ Δ , and *STE12* complemented *C. lusitaniae* strains. A morphology change (polarized growth) is evident in wildtype diploid strains grown on PDA medium starting at 12 h, while spore formation is apparent at 18-36 h. In the *ste12* $\Delta/ste12$ Δ mutant, both sporulation and morphology change are absent. **d**, Global transcriptional profile of meiosis in *C. lusitaniae* showing induced genes (yellow) and repressed genes (blue). *C. lusitaniae* diploid a/a cells (RSY432) were grown on PDA (sporulating) medium and expression changes compared to those on YPD (non-sporulating) medium. Genes changing more than 4-fold in expression are shown.



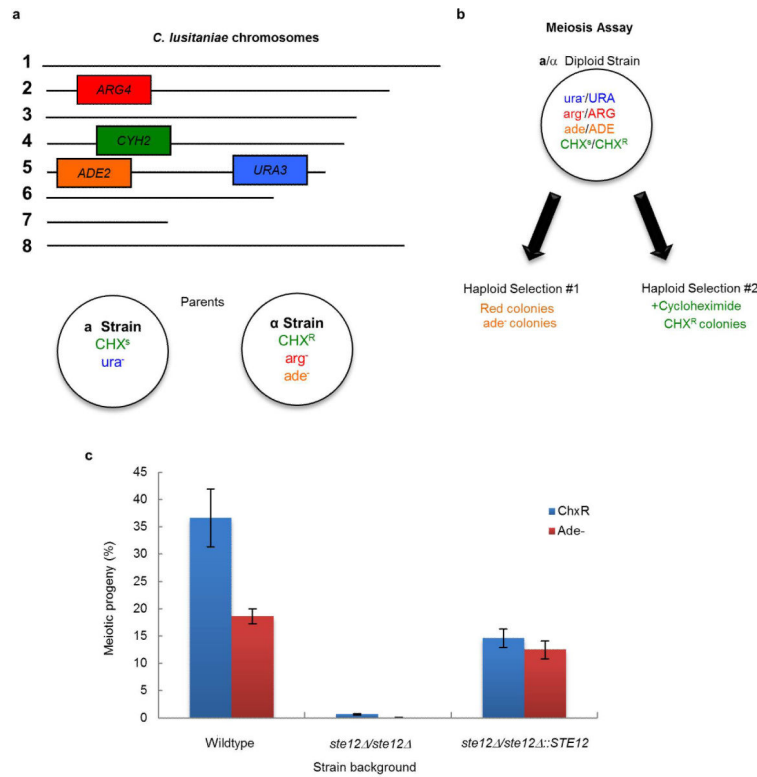
Extended Data Figure 3. Transcriptional profiling of *C. lusitaniae* wildtype and *ime2* mutants during mating and meiosis

a, Full profile of wildtype and *ime2 /ime2* strains during meiosis indicates that many transcriptional changes occur in *ime2 /ime2* mutants as in wildtype strains. **b**, Analysis of cell cycle regulating genes during *C. lusitaniae* meiosis. Several cell cycle genes are induced in wildtype cells undergoing meiosis but not in *ime2 /ime2* mutants (e.g., *APC4*, *CDC3*, *CDC10*, and *CDC14*). **c**, Comparative expression of early (*IME2*, *IME4*, *SPO11*), middle (*REC102*, *CDC3*, *SPS4*, *SPS1*, *NDT80*, *SWM1*) and late (*DIT1*, *DIT2*) meiosis genes. **d**, In contrast to the meiotic profiles, the mating profiles of wildtype and *ime2* strains were very similar. **e**, Comparison of meiosis genes induced in wildtype and *ime2* mutants.



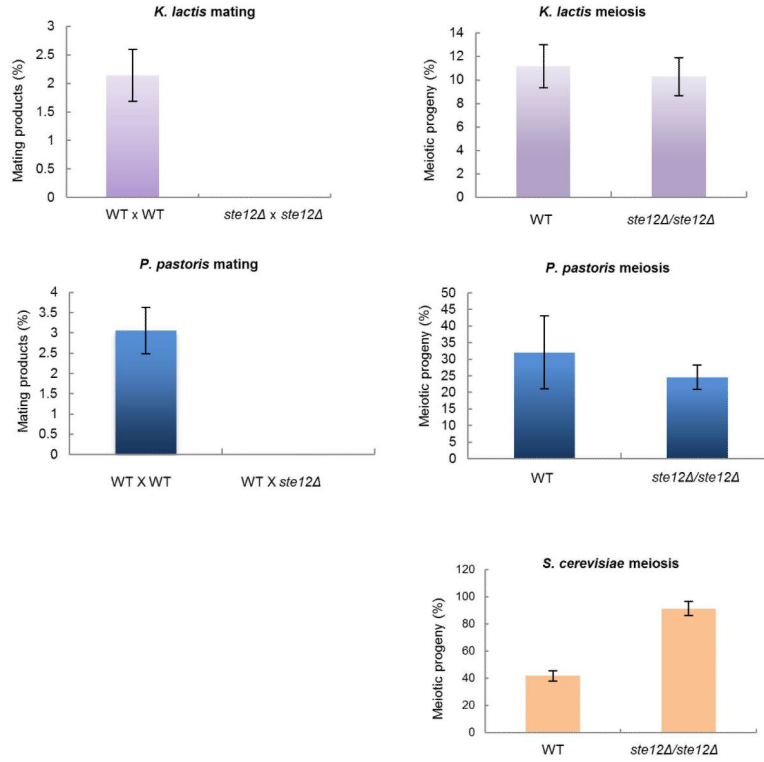
Extended Data Figure 4. Reintegration of *IME2* restores mating efficiency

IME2 was reintegrated at the endogenous locus in an *ime2* mutant (RSY437). Mating frequency was quantified by monitoring the formation of prototrophic products from auxotrophic parents. WT cross, RSY411 x RSY284, *ime2* mutant cross, RSY406 x RSY437, *IME2* complemented cross, RSY406 x CAY5022. Differences between the WT cross and the *ime2* mutant cross, and between the *IME2* complemented cross and the *ime2* mutant cross were both significant. (n=7, p < 0.001, Kruskal Wallis test). Data are representative of mean +/- s.e.m.



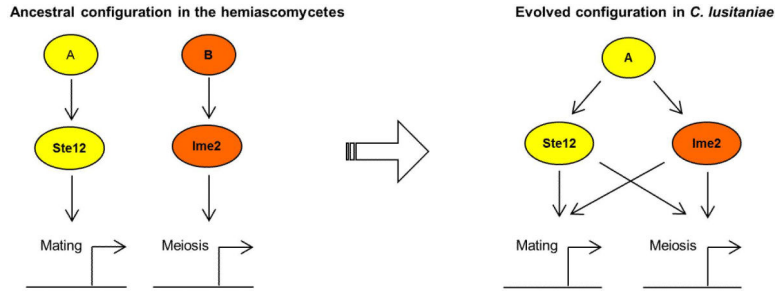
Extended Data Figure 5. Schematic of genetically marked *C. lusitaniae* strains and control of meiosis by *STE12*

a. *C. lusitaniae* mating experiments were performed between RSY284 (**a** strain) and RSY411 (**α** strain) and mating products selected based on auxotrophic markers. **b.** The **a/α** diploid strain RSY432 was induced to undergo meiosis on PDA medium and meiotic progeny identified by their red color on YPD medium (*ade* colonies) or by growth on medium containing cycloheximide (CHX resistant colonies). **c.** Diploid **a/α** strains of *C. lusitaniae* were incubated on PDA medium for 3 days and analyzed for the frequency of formation of meiotic progeny. Two independent *ste12* mutants were constructed in the **a/α** background and tested for meiotic progeny using both the *CHXR* and *ADE2* markers. Mutants lacking *STE12* were unable to undergo meiosis to produce haploid progeny, while reintegration of *STE12* into the mutant background restored meiosis. Differences between both wildtype strains and *ste12* mutants, and between *ste12* mutants and *STE12*-complemented strains were significant ($n=3$, $p < 0.05$, student's t test, two tailed). Data representative of mean \pm s.e.m.



Extended Data Figure 6. Analysis of STE12 function in mating and meiosis in diverse hemiascomycete species

The *STE12* gene was deleted from haploid and diploid strains of *K. lactis*, *P. pastoris*, and *S. cerevisiae*. The resultant strains were tested both for mating competency and the formation of meiotic progeny. Whereas deletion of *STE12* blocked mating in haploid strains of all three species, loss of *STE12* from diploid a/α strains did not have a significant effect on the formation of meiotic progeny. Thus, *C. lusitanae* is unique among the hemiascomycete species tested in that *STE12* is essential for meiosis only in this species. *K. lactis* mating and meiosis, n=2, data combined for 3 independent mutants. *P. pastoris* mating, n=3. *P. pastoris* meiosis n=4. *S. cerevisiae* meiosis n=3. All data presented as mean +/- s.e.m.



Extended Data Figure 7. Rewiring of the genetic programs that control sexual reproduction in hemiascomycetes

In many hemiascomycete species, including the model yeast *S. cerevisiae*, mating and meiosis are controlled by two distinct transcriptional programs with *STE12* as the master regulator of mating and *IME2* as a key regulator of meiosis. However, in the opportunistic pathogen *C. lusitaniae*, *STE12* has retained its role in regulating mating, but has also acquired control over meiosis. Similarly, *C. lusitaniae* *IME2* has a conserved role in regulating mating, but also has a role in promoting mating. The transcriptional programs controlling these two processes have therefore fused in *C. lusitaniae*, perhaps to facilitate a transient diploid state and the more efficient return to the predominant haploid state.